Electronic Supplementary Information

Reusable Magnetic Graphene Oxide based Anion Exchanger for the Separation and Removal of Anionic Dyes

Poonam Kumari, [a,b] Disha, [a,b] Raj Rani, [a,b] Manoj K. Patel, [b,c] Sunita Mishra, [a,b] Sandeep Singhai, [b,d] Manoj K. Nayak, [a,b*]

[a] Materials Science and Sensor applications, *CSIR-Central Scientific Instruments Organisation (CSIR-CSIO), Sector 30-C, Chandigarh- 160030, India.*

[b] *Academy of Scientific and Innovative Research (AcSIR), Ghaziabad, Uttar Pradesh- 201 002, India.*

[c] *Manufacturing Science and Instrumentation, CSIR-Central Scientific Instruments Organisation. Sector 30-C, Chandigarh-160030, India.*

[d] *Centre for Advanced Radiation Shielding and Geopolymeric Materials,CSIR-Advanced Materials and Processes Research Institute, Bhopal- 462026, India.*

**Corresponding author E-mail: mknayak@csio.res.in*

Table S1. Elemental composition analysis of GO, MGO, NGO, and NMGO using high resolution XPS spectra.

Chemical states	**Atomic Concentration (%)**			
	GO	MGO	NGO	NMGO
C 1s	67.98	36.03	71.01	36.18
O 1s	32.02	44.36	26.65	42.72
Fe 2p	-	19.62	-	18.88
N 1s	-	-	3.47	2.22

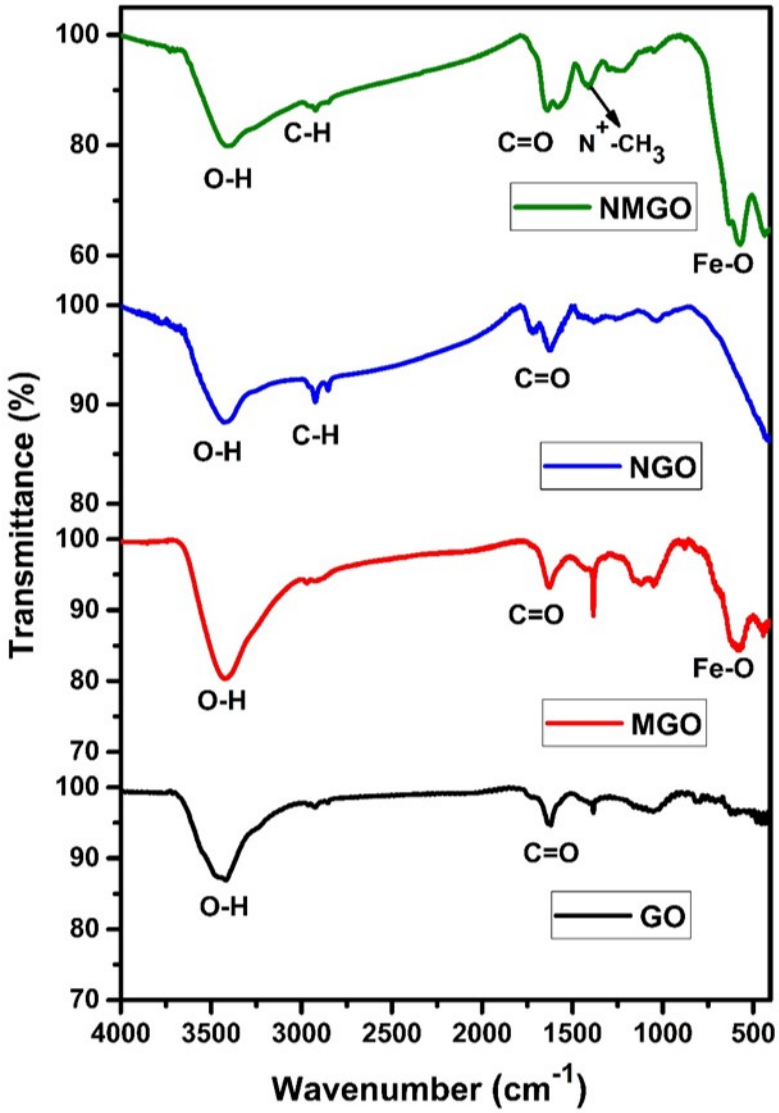

Fig. S1. FTIR spectra for GO, MGO, NGO, and NMGO

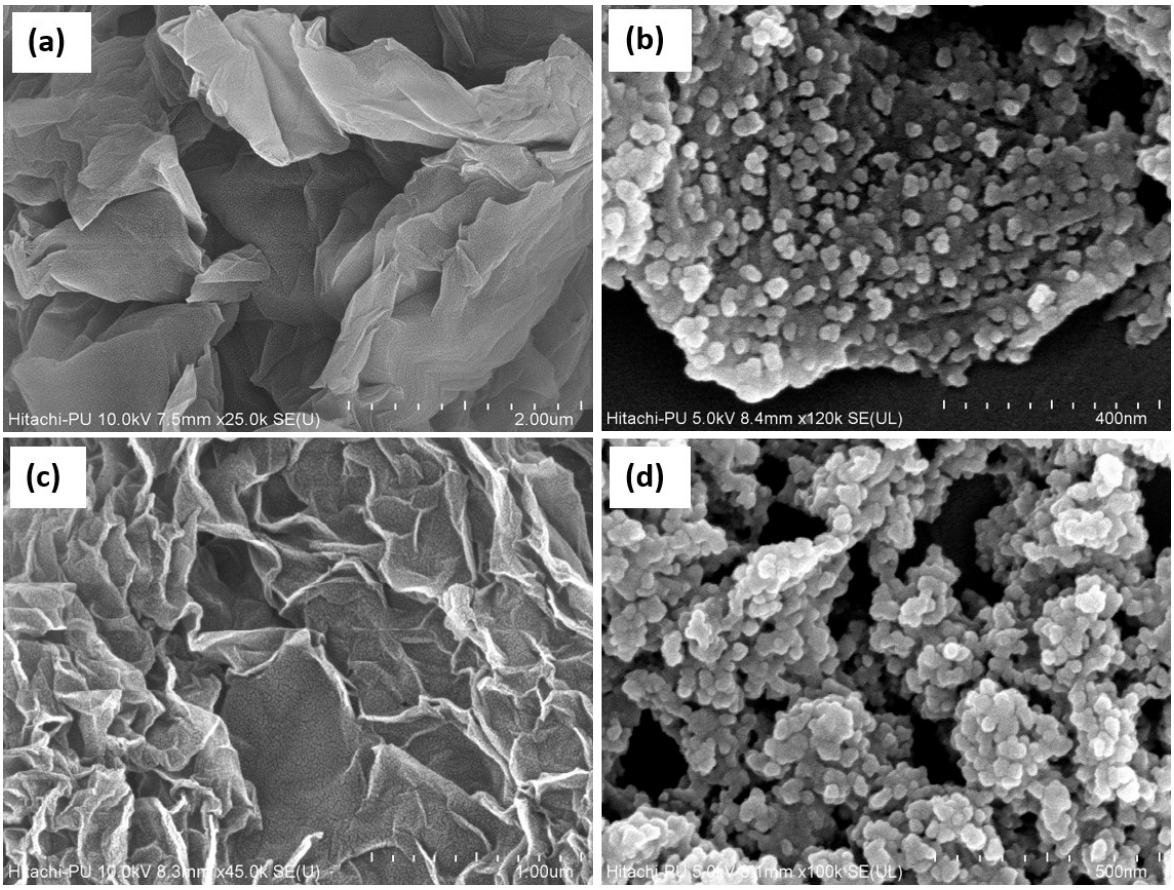

Fig. S2. FESEM images for (a) GO, (b) MGO, (c) NGO, and (d) NMGO.

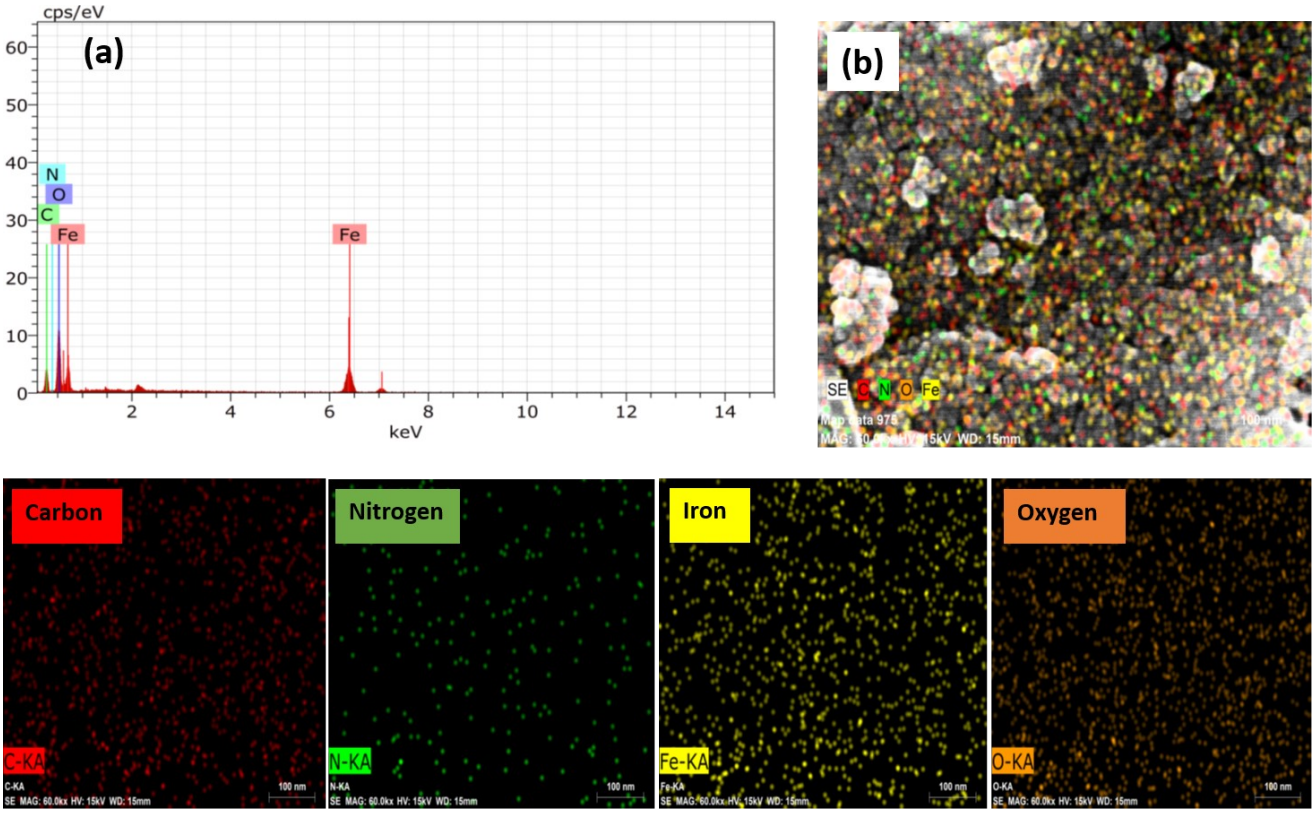

Fig. S3. EDS and elemental mapping of NMGO.

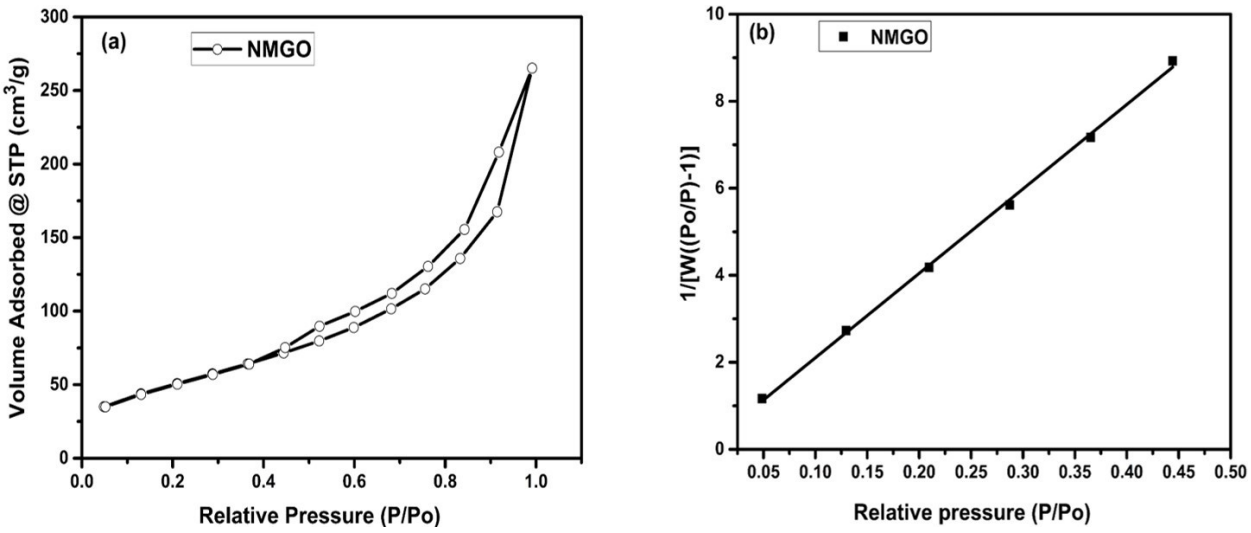

Fig. S4. (a) Brunauer-Emmett-Teller (BET) Nitrogen (N_2) adsorption-desorption isotherms of NMGO and (b) The fitting curve of the BET surface area of NMGO.

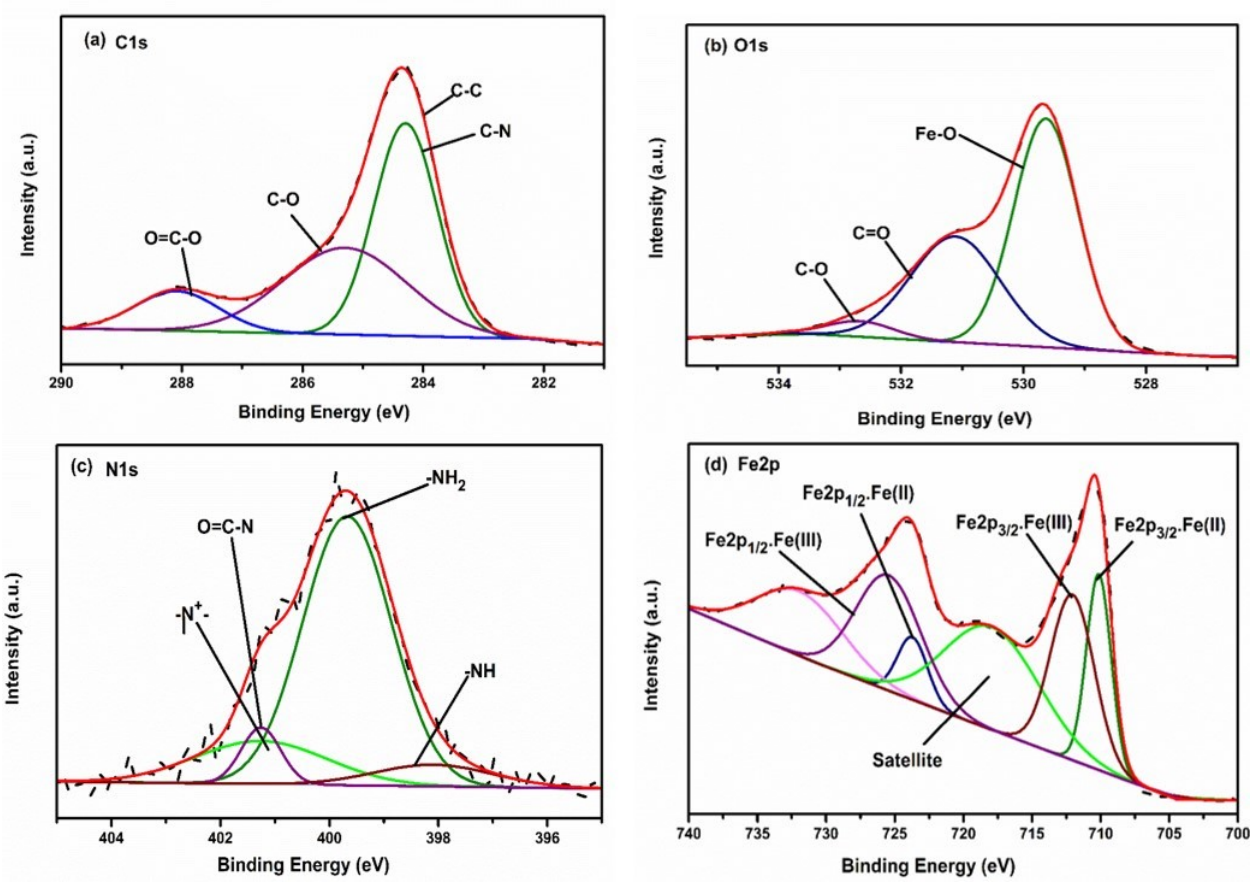

Fig. S5. High resolution XPS spectra of (a) C1s, (b) O1s, (c) N1s, and (d) Fe2p of NMGO.

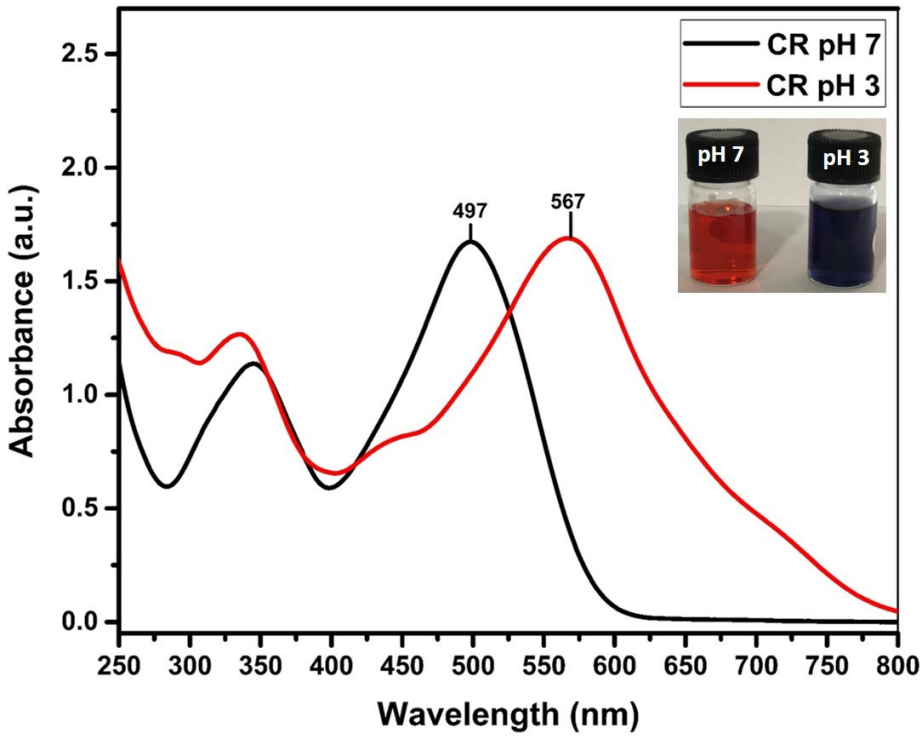

Fig. S6. UV-Vis spectra of Congo red at pH 7 and pH 3 with maximum absorption at 497 and 567 nm.

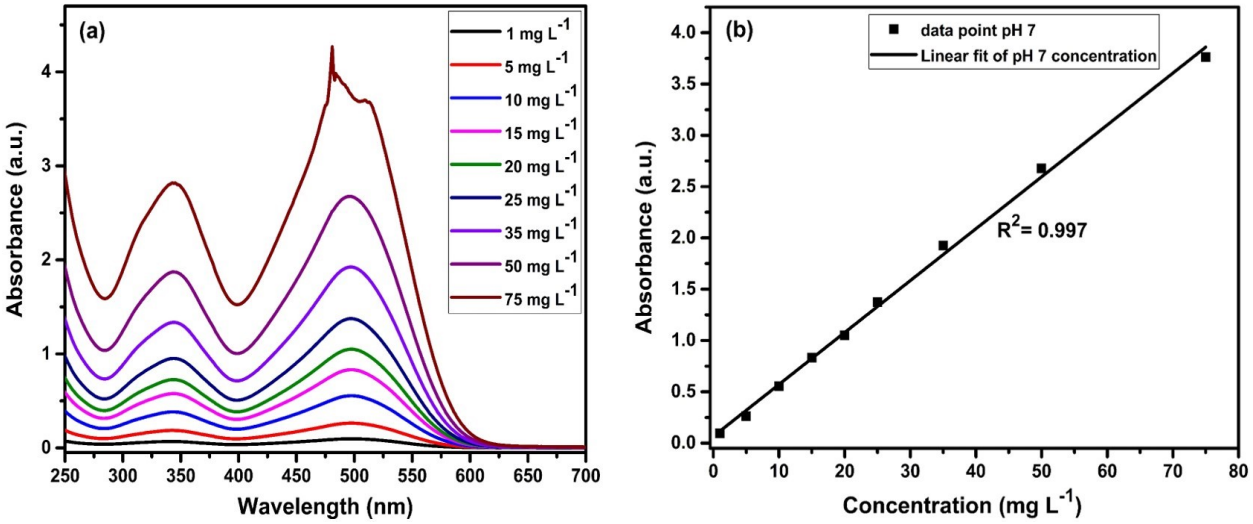

Fig. S7. (a) The UV-Vis spectra of the Congo red in an aqueous solution at different concentrations at pH 7 with a maximum absorption of 497 nm at rt. (b) Calibration curve of different concentrations at pH 7 for the Congo red.

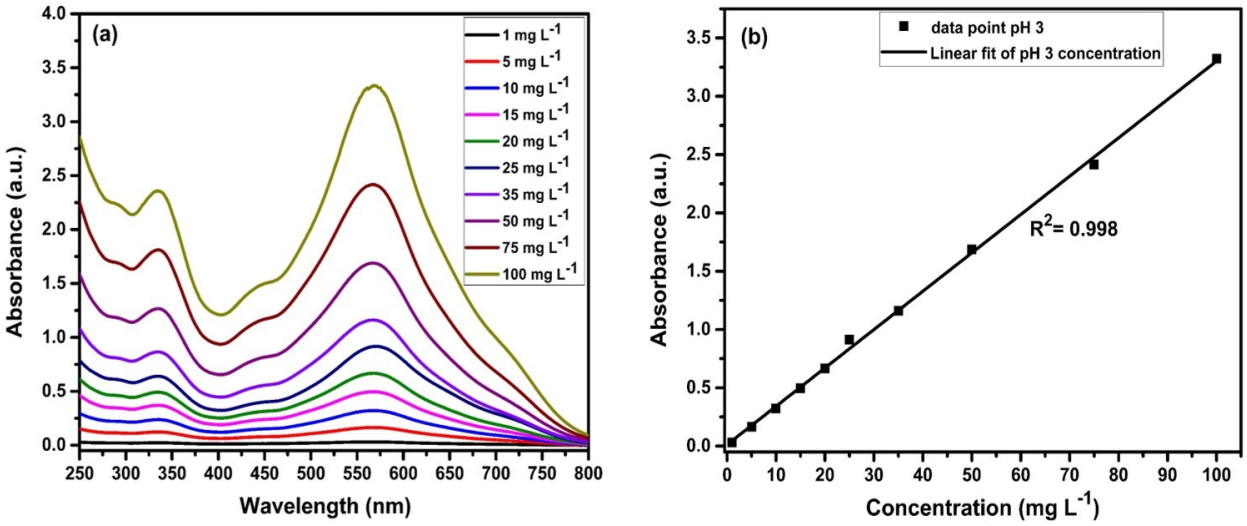

Fig. S8. (a) The UV-Vis spectra of Congo red in an aqueous solution at different concentrations at pH 3 with a maximum absorption of 567 nm at rt. and (b) Calibration curve of different concentrations at pH 3 for the Congo red.

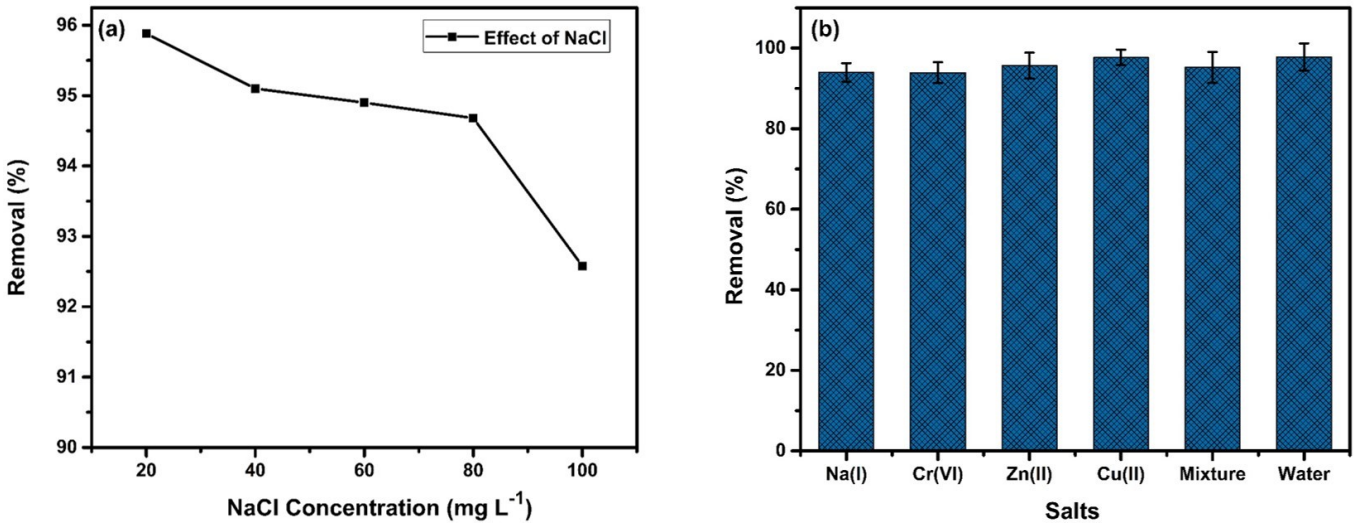

Fig. S9. (a) Effect of NaCl concentration on adsorption of Congo red onto NMGO (dye concentration 50 mg L^{-1}) (b) Effect of different metal salts on the adsorption of Congo red onto NMGO.

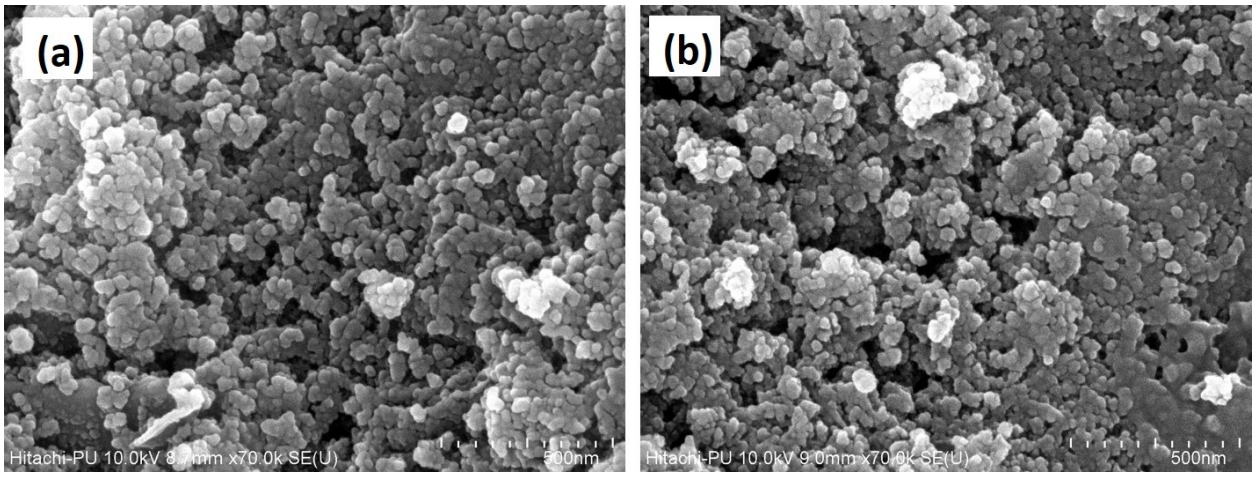

Fig. S10. FESEM images of (a) NMGO before and (b) after adsorption of Congo red.

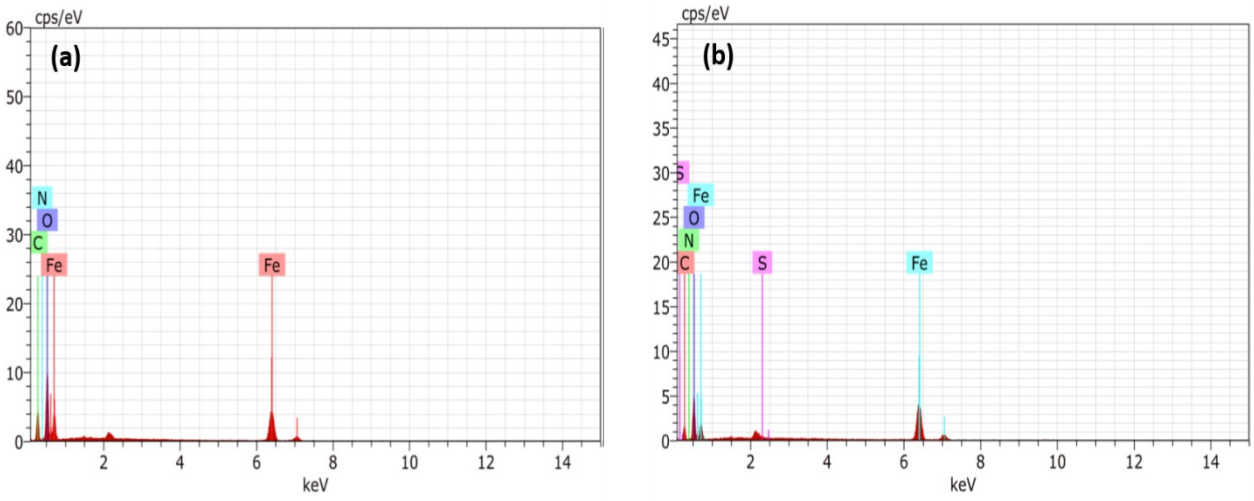

Fig. S11. EDS images of (a) NMGO before and (b) after adsorption of Congo red.

Table S2. EDS analysis of NMGO before and after adsorption of Congo red.

Atom (%)	**NMGO**	**NMGO-CR**
Carbon	36.75	37.28
Oxygen	32.67	31.88
Iron	24.39	29.24
Nitrogen	1.67	1.40
Sulfur	-	0.21

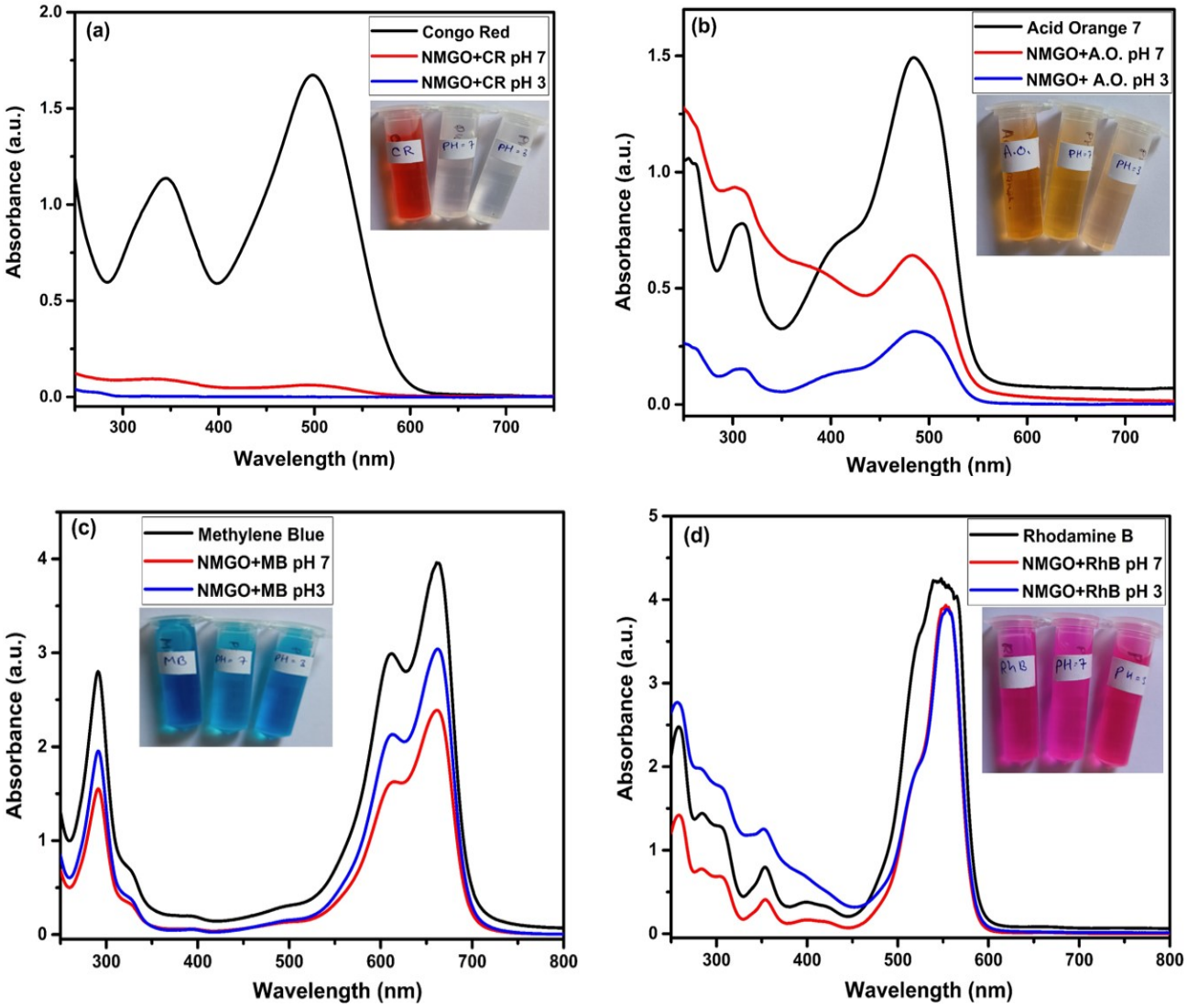

Fig. S12. Dye selectivity study with the NMGO using (a) Congo red, (b) Orange acid 7, (c) Methylene blue, and (d) Rhodamine B at neutral and acidic pH (@dye concentration- 25 mg L^{-1}; adsorbent dosages- 2 mg/10 mL; contact time- 150 min.)

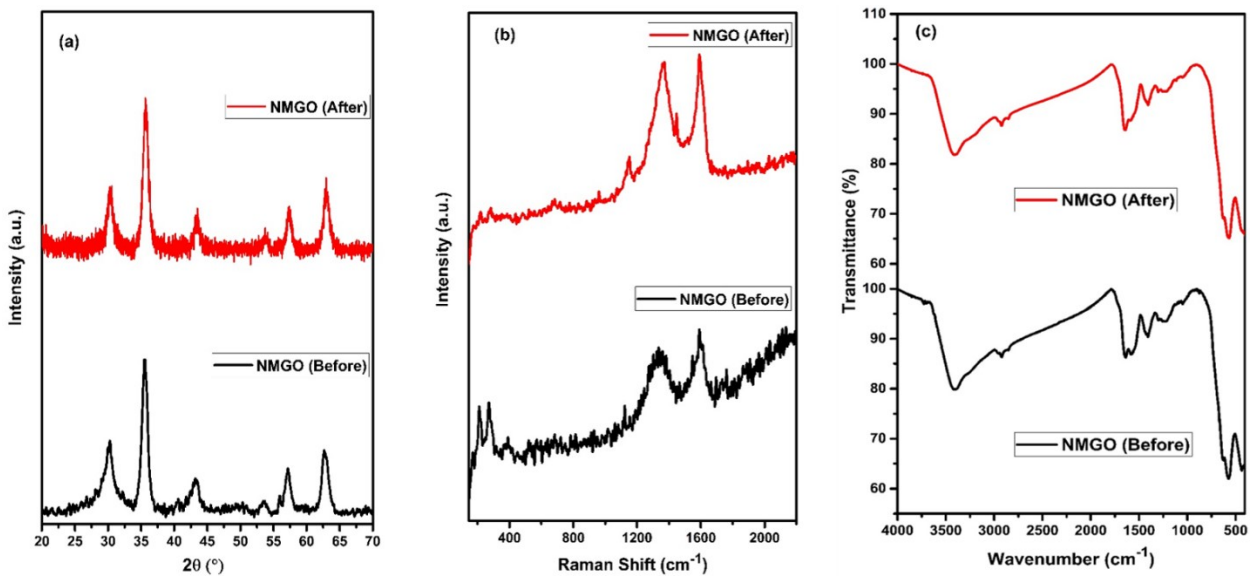

Fig. S13. (a) XRD, (b) Raman, and (c) FTIR of NMGO prior to the adsorption of Congo red and its subsequent regeneration.